Sustainable Food Technology

ROYAL SOCIETY OF CHEMISTRY

PAPER

View Article Online
View Journal

Cite this: DOI: 10.1039/d5fb00817d

Sustainable biopolymeric films of gelatin/kappa-carrageenan reinforced with jackfruit-derived cellulose nanocrystals for mushroom packaging

Ajitkumar Appayya Hunashyal,[a] Saraswati P. Masti, *[a] Lingaraj Kariyappa Kurabetta,[b] Manjushree Nagaraj Gunaki,[a] Jennifer P. Pinto,[b] Priyadarshini,[c] Shiddalingesh G. Havanur,[c] Bhagyalakshmi A. Sheeparamatti,[c] Priyanka Baburao[c] and Ravindra B. Chougale[c]

In this research, cellulose nanocrystals were derived from jackfruit peel (JCNCs) through the acid hydrolysis method and analysed using TEM, SEM-EDS, DLS and XRD techniques. The mean size of prepared spherical cellulose nanocrystals was 97.56 nm. These characterised JCNCs were then integrated into a gelatin/kappa-carrageenan (GK) matrix at increasing concentrations to fabricate biopolymer films labelled as GKC-1, GKC-2, GKC-3 and GKC-4. The prepared films were extensively characterized, including assessments of UV-blocking capability, transparency, mechanical strength, FTIR, XRD analyses, water vapor permeability (WVP), oxygen permeability (OP), water solubility (WS), moisture retention capacity (MRC), SEM-EDS imaging, soil burial biodegradability testing and antioxidant activity. The addition of JCNCs notably modified the structural and functional attributes of the GK films. The optimized GKC-4 film exhibited enhanced performance in several critical areas compared to the control film (GK), such as a 30.5% reduction in WVP, an 87% increase in tensile strength, a 182.264% and 151.447% rise in DPPH and ABTS antioxidant activities and a 39.19% decrease in the degradation rate during the soil burial test. Furthermore, packaging experiments were conducted with button mushrooms stored at 4 °C for 12 days. The findings indicated that the GKC-4 film significantly minimized weight loss to 9.21 ± 0.02% and retained pH stability at a 6.61 ± 0.15 pH value compared to unpackaged samples and commercial polyethene films. These results highlight the potential of JCNC-reinforced biopolymer films as sustainable and functional alternatives for active food packaging.

Received 31st October 2025
Accepted 2nd February 2026

DOI: 10.1039/d5fb00817d

rsc.li/susfoodtech

Sustainability spotlight

This study presents a sustainable approach to valorize jackfruit peel waste into high-value cellulose nanocrystals (JCNCs) for developing eco-friendly food packaging films. By reinforcing gelatin/kappa-carrageenan biopolymers with JCNCs, the resulting films exhibit superior mechanical strength, barrier performance, and antioxidant activity, while retaining biodegradability. The optimized GKC-4 film effectively prolonged the shelf life of button mushrooms, reducing weight loss and retaining pH stability during cold storage. This work exemplifies a circular bioeconomy model by converting agricultural waste into functional materials, offering a green alternative to petroleum-based plastics for active packaging applications and promoting sustainability in the food industry.

1 Introduction

Food is universally regarded as one of the most fundamental necessities for human survival, alongside air and water. Unfortunately, a significant amount of food is wasted due to various factors, including short shelf life, oxidative degradation, exposure to harmful UV rays, moisture and microbial contamination.[1] The widespread use of petroleum-based packaging materials exacerbates this issue, posing serious risks to human health, animal welfare and environmental sustainability.[2] The COVID-19 pandemic significantly escalated plastic pollution through increased use of single-use plastics and disruptions in recycling efforts. This highlights the urgent need for innovative solutions like biodegradable plastics to address the growing plastic waste crisis.[3,4] In contrast, bio-based packaging materials have emerged as a highly effective and eco-friendly alternative, addressing many of these challenges.[5] These innovative materials not only enhance food preservation but also exhibit a superior degradation rate, thereby minimizing environmental impact and significantly reducing the carbon footprint.[6] We can take a meaningful step towards creating a greener, healthier

[a]Department of Chemistry, Karnatak Science College, Dharwad-580001, Karnataka, India. E-mail: dr.saraswatimasti@yahoo.com
[b]Indian Institute of Packaging, Bengaluru-562132, Karnataka, India
[c]Department of Chemistry, Karnatak University, Dharwad-580003, Karnataka, India

planet by replacing conventional packaging with bio-based solutions.[7,8] Bioplastics encompass a diverse group of bio-obased materials, biodegradable materials or a combination of both. Biobased plastics are made partially or entirely from renewable biological sources, while biodegradable plastics break down naturally into carbon dioxide and water through the activity of microorganisms in the environment.[3,9,10] Bioplastics offer numerous benefits, including reduced environmental impact due to their renewable origins and lower greenhouse gas emissions. They provide excellent protection against food spoilage, are recyclable and/or biodegradable and exhibit comparable or superior mechanical properties to conventional plastics. Additionally, they align with consumer preferences for sustainable packaging, boosting market appeal for eco-conscious products.[3,11]

Natural and biodegradable polymers are promising and sustainable alternatives to conventional plastics for food packaging, offering eco-friendly solutions with added benefits.[12] The incorporation of functional ingredients, such as potent antioxidants and antimicrobial agents, enhances food quality, appearance and shelf life, making these materials highly versatile.[13] Polysaccharides exhibit exceptional oxygen and aroma barrier properties due to their hydrophilic nature and ability to form strong hydrogen bonds, while protein-based films shine in providing superior gas barrier properties but fall short as effective water barriers.[13–16] Interestingly, blending proteins with polysaccharides creates a synergistic effect, significantly improving the gas barrier performance of these innovative films, which hold great potential for revolutionizing the food packaging industry.[13] Among polysaccharides, kappa-carrageenan (KC) has emerged as a versatile hydrocolloid sourced from red algae, renowned for its excellent water solubility, antioxidant potential and robust gel-forming capability in the presence of specific cations.[17,18] Despite these attributes, its limited mechanical durability and inadequate barrier properties restrict its independent use in packaging applications.[13,19,20] Proteins like gelatin (GL), a denatured biopolymer obtained from collagen hydrolysis, act as complementary partners to polysaccharides by offering exceptional film-forming, gelling and antioxidant properties, alongside enhanced gas and aroma barrier functionalities.[13,20,21] The strategic blending of polysaccharides such as KC with proteins like GL creates a synergistic composite, effectively combining the strengths of both materials. Notably, a 50 : 50 KC/GL composite has demonstrated outstanding physical and functional properties, positioning it as an innovative and sustainable choice for advanced active food packaging.[20,22]

Cellulose nanocrystals (CNCs) are gaining recognition as valuable components for active food packaging, owing to their biodegradable nature, compatibility with biological systems and superior mechanical characteristics.[23,24] These nanocrystals can be extracted from agricultural byproducts and incorporated into biocomposite films to enhance the barrier, mechanical, and thermal properties of packaging materials.[24] CNCs also function as vehicles for bioactive substances, including antioxidants and antimicrobials, thereby prolonging food shelf life and enhancing quality.[25] Modifying the surface chemistry of CNCs allows for the addition of new functionalities, broadening their potential uses in food packaging.[26] Moreover, CNCs can be utilized as low-calorie substitutes for carbohydrate additives in food items, serving as thickeners, flavor carriers and suspension stabilizers.[23] Prior research has demonstrated that incorporating nanocellulose materials can substantially enhance the mechanical, barrier and functional characteristics of films produced from natural polymers such as chitosan, alginate and zein.[27–29] Introducing CNCs or CNFs (carbon nanofibers) into biopolymer films boosts tensile strength, decreases water vapor and oxygen permeability and improves light barrier properties.[27,28] Additionally, films reinforced with nanocellulose show enhanced antimicrobial activity and antioxidant properties, making them ideal for active food packaging applications.[28,29] The improved performance of these nanocomposite films is attributed to the establishment of hydrogen bonds between nanocellulose and the polymer matrix and the filling effect of nanocellulose particles.[28,29] These developments in nanocellulose-based food packaging materials correspond with the increasing demand for sustainable and biodegradable alternatives to traditional plastics.[26]

The present investigation focuses on the extraction of cellulose nanocrystals (CNCs) from jackfruit biowaste through an economically viable acid hydrolysis technique. These CNCs are subsequently incorporated into biopolymer matrices comprising gelatin and κ-carrageenan at various concentrations using a straightforward film casting approach. CNCs are postulated to possess remarkable attributes, including superior gas barrier properties, enhanced mechanical robustness and biodegradability, making them prime candidates for eco-friendly food packaging solutions.[30] Nevertheless, obstacles such as production scalability and quality consistency have impeded their widespread adoption.[31] The primary aim is to fabricate biodegradable packaging films exhibiting improved mechanical, barrier and functional characteristics.

2 Materials and methods

2.1 Materials

Gelatin (CAS No. 900-70-8) was sourced from Sisco Research Laboratories Pvt. Ltd, while kappa-carrageenan (CAS RN: 11114-20-8) was obtained from Tokyo Chemicals Industry Co. Ltd, Bangalore. Glycerol, with a purity of 98% (CAS RN: 56-81-5), was acquired from ACE Rasayan Company Pvt. Ltd, Dharwad. Fresh jackfruit peels were collected from street vendors at the local market. Throughout the experiment, double-distilled water and ethanol were utilized to ensure the highest level of purity and reliability.

2.2 Methods

2.2.1 Preparation of jackfruit-derived cellulose nanocrystals. The synthesis of jackfruit-derived cellulose nanocrystals (JCNCs) was carefully conducted following the protocol outlined by C. Trilokesh *et al.*[32] Initially, shade-dried jackfruit waste was ground into a fine powder using a pestle and mortar to increase its surface area for further processing. 30 g of this

powder was then subjected to solvent extraction by soaking it in water, followed by ethanol for four hours each, effectively removing soluble impurities and improving the overall purity of the material. The extracted residue was treated with sodium chlorite ($NaClO_2$) for bleaching, with the pH adjusted between 3 and 4 and the temperature maintained at 70 °C. This step was essential for removing lignin and hemicellulose, enriching the cellulose content. The bleached material was subsequently treated with a sodium hydroxide (1 M NaOH) solution at 60 °C to eliminate residual impurities and enhance its chemical reactivity. Afterwards, the material was thoroughly washed with water at 60 °C to neutralize any remaining alkali and prepare it for the subsequent process. Acid hydrolysis was then carried out using sulfuric acid (65 wt%, 1 : 9 g mL^{-1} H_2SO_4), targeting the amorphous regions of the cellulose to produce highly crystalline nanocellulose. The hydrolyzed mixture was centrifuged at 3000 rpm to separate the nanocrystals effectively. Finally, rotary evaporation was used to concentrate and purify the suspension, resulting in high-quality JCNCs.

2.2.2 Optimization of GK biopolymeric films. Initially, gelatin and κ-carrageenan were combined in three distinct ratios (1 : 3, 1 : 1, and 3 : 1) and placed into separate beakers. A homogeneous solution was prepared by blending the components in 150 mL of double-distilled water in a 250 mL beaker using a magnetic stirrer for 2 hours. The resulting solution was then carefully cast onto Petri dishes and allowed to dry overnight at 40 °C. Once dried, the films were gently peeled off for analysis. Among the tested ratios, the 1 : 1 blend exhibited superior mechanical properties, making it the optimal choice for fabricating gelatin/kappa-carrageenan/JCNC (GKC) nanocomposite films.[33,34]

2.2.3 Fabrication of GKC nanocomposite films. To the optimized 1 : 1 gelatin/κ-carrageenan (GK) blend, jackfruit-derived cellulose nanocrystals (JCNCs) were incorporated at varying concentrations based on the polymeric weight: 1%, 3%, 5% and 7%, labelled as GKC-1, GKC-2, GKC-3 and GKC-4, respectively. The mixtures were stirred continuously for 4 hours using a magnetic stirrer to ensure the formation of a homogeneous solution, employing the solution casting method.[35] The prepared solutions were carefully poured onto Petri dishes and dried overnight at 40 °C. Once dried, the nanocomposite films were gently peeled off and stored in a desiccator to preserve their properties for subsequent characterization.[36,37]

2.3 Characterization techniques

2.3.1 Characterizations of jackfruit derived cellulose nanocrystals (JCNCs). Characterizations of JCNCs were carried out by TEM, SEM, XRD, and DLS. For TEM, diluted JCNCs were drop-cast onto carbon-coated copper grids and imaged to determine size and morphology. SEM analysis involved mounting JCNC samples on stubs, sputter-coating with a conductive layer, and imaging to assess surface morphology and aggregation. Powder XRD was performed with Cu Kα radiation over an appropriate 2θ range to confirm crystalline cellulose and identify characteristic reflections (*e.g.*, near the (200) plane). DLS measurements were conducted on JCNC suspensions in water at 25 °C to obtain hydrodynamic size distributions (Z-average) and the PDI, indicating nanoscale dispersion and aggregation tendency.

2.3.2 Fourier transform infrared (FTIR) spectroscopic analysis. The molecular interactions and functional groups present in the active films were investigated using an Attenuated Total Reflectance-Fourier Transform Infrared (ATR-FTIR) spectrometer (Shimadzu, Japan). The spectra were recorded in the range of 4000–400 cm^{-1} with a resolution of 4 cm^{-1} to identify chemical bonds and structural changes.[38]

2.3.3 X-ray diffraction (XRD) analysis. The crystalline and amorphous phases of the films were analyzed using an X-ray diffractometer (DMAX 2500, Rigaku, Japan). The instrument was operated at 40 kV and 30 mA, scanning over a 2θ range of 5–80° at a speed of 5° min^{-1} to determine the crystallinity and structural properties of the films.[39]

2.3.4 Surface morphology examination. The surface morphology of the active films was examined using a Scanning Electron Microscope (SEM, JEOL JSM-6360 SEM-EDS). This analysis provided detailed insights into the surface structure, homogeneity, and potential defects or irregularities in the films.[40]

2.3.5 Mechanical properties. The mechanical properties of the films, including tensile strength and elongation at break, were evaluated using a universal testing machine following the ASTM D 882-88 standard. Film strips measuring 25 × 100 mm^2 were tested with 50 mm grip separation at a cross-head speed of 5 mm min^{-1}. The average values from three replicates were reported.[41]

2.3.6 UV-light barrier properties. The UV-light barrier properties of the active films were analyzed to determine their ability to block ultraviolet (UV) radiation and transmit visible light. A UV-visible spectrophotometer (PerkinElmer LAMDA 365) was used to measure the transmittance spectra of the films. The UV-blocking efficiency and visible light transmission were calculated using the following equations:

$$\text{Transparency (T600): } \text{T600} = \frac{-\log(\%T)}{b}$$

$$\text{UV-A blocking } (\%) = 100 - \frac{\int_{320}^{400} T(\lambda)\mathrm{d}\lambda}{\int_{320}^{400} \mathrm{d}\lambda}$$

$$\text{UV-B blocking } (\%) = 100 - \frac{\int_{280}^{320} T(\lambda)\mathrm{d}\lambda}{\int_{280}^{320} \mathrm{d}\lambda}$$

Here, b represents the film's thickness, $T(\lambda)$ denotes the average wavelength transmittance, and $d\lambda$ signifies the bandwidth.[42]

2.3.7 Water vapor permeability (WVP) and oxygen permeability (OP). Water vapor permeability (WVP) was measured using a modified gravimetric method. Film samples (4 × 4 cm^2)

were sealed onto glass tubes containing anhydrous calcium chloride at 0% relative humidity (RH) and placed in a desiccator with distilled water (100% RH) at room temperature. The weight change was recorded every 24 hours for three days. WVP was calculated using

$$\mathrm{WVP} = \frac{\mathrm{WVTR}}{P} \times (\mathrm{RH}_1 - \mathrm{RH}_2) \times X$$

where WVTR is the water vapor transmission rate, X is the film thickness, P is the saturation vapor pressure at 25 °C, and RH_1 and RH_2 are the relative humidities.[43]

Oxygen permeability (OP) was determined by sealing film samples onto glass tubes, weighing them, and placing them in a desiccator with silica gel. The weight change was recorded every 24 hours for three days. OP was calculated using

$$\mathrm{OTR} = \frac{\mathrm{Slope}}{A}$$

where OTR is the oxygen transmission rate, A represents the effective exposed area of the film (m^2), and Slope corresponds to the rate of weight change per unit time obtained from the linear regression of mass gain *versus* time.

$$\mathrm{OP} = \frac{\mathrm{OTR}}{\Delta P} \times X$$

where X is the film thickness and ΔP is the oxygen partial pressure difference across the film.[44]

2.3.8 Moisture absorption (MA) and water solubility (WS). Moisture absorption (MA) was determined following ASTM D570-98. Film samples (3×3 cm^2) were weighed before (M_i) and after (M_f) drying at 105 °C for 24 hours. MA was calculated as[45]

$$\text{Moisture absorption } (\%) = \frac{M_i - M_f}{M_i} \times 100$$

Water solubility (WS) was assessed by drying film samples at 105 °C for 24 hours to obtain the initial weight W_i. The samples were then immersed in distilled water for 24 hours, dried again, and weighed (W_f). WS was calculated as

$$\text{Water solubility } (\%) = \frac{W_i - W_f}{w_i} \times 100$$

2.3.9 Water contact angle (WCA) measurements. The film's surface wettability was evaluated using a water contact angle analyzer (DMs-401). A 1 μL droplet of distilled water was placed on the film surface, and the static contact angle was measured. The average value from five measurements was reported.

2.3.10 Soil burial degradation test. The biodegradability of the films was assessed through a soil burial test. Film samples (2×2 cm^2) were dried at 100 °C, weighed (W_i), and buried 10 cm deep in soil. After a specified period, the samples were retrieved, cleaned, dried, and weighed (W_f) to determine the percentage weight loss:

$$\text{Soil burial degradation rate } (\%) = \frac{W_i - W_f}{W_i} \times 100$$

2.3.11 Button mushroom packaging studies. Fresh button mushrooms (*Agaricus bisporus*) of marketable quality, uniform size and maturity and free from visible defects were selected from the local market. Adhering soil was carefully removed by dry brushing without washing. The samples were randomly allocated to one of four packaging treatments: unpackaged, GK control film, GKC-4 film and commercial polyethene film. Storage was conducted at 4 °C in a refrigerated chamber, and sampling was performed on days 0, 3, 6, 9, and 12.

2.3.12 Weight loss (%) determination. The initial weight of each package (W_0) was recorded using a calibrated analytical balance (±0.01 g) immediately after packaging. At each sampling interval, the weight of the package (W_t) was measured after removal from storage and equilibration to room temperature for approximately 15 minutes. The percentage of weight loss was calculated using the equation:

$$\text{Weight loss } (\%) = \frac{W_t - W_0}{W_0} \times 100$$

2.3.13 pH measurement. For pH determination, approximately 2 g of button mushroom sample was homogenized with distilled water at a 1 : 10 (w/v) ratio in a sterile homogenizer. After allowing the homogenate to settle, the pH of the supernatant was measured at room temperature using a bench-top pH meter that was calibrated. The electrode was rinsed and blotted between successive measurements. Three readings were taken for each homogenate, and the mean value was reported as the pH for each replicate. All procedures were carried out under aseptic conditions.

2.3.14 Sensory evaluation of packaged button mushrooms. All the packaged button mushrooms were evaluated on a 10-point scale, 10 being most desirable. Sensory evaluations were conducted on days 0, 3, 6, 9, and 12 for appearance, texture, odour, and overall acceptability. At each interval, samples were presented to panellists in randomised order under neutral lighting and in a neutral environment to minimize bias. For each attribute and time point, scores were recorded as mean ± standard deviation, and trends over time among packaging types were interpreted based on these summary statistics.

2.3.15 Statistical analysis. The replicated experimental units used for measuring the attributes of the films were measured for individually prepared films in triplicate. Using the SPSS statistical analysis software for Windows, a one-way analysis of variance (ANOVA) was carried out, and each mean property value's significance ($p < 0.05$) was ascertained using Tukey's test.

3 Results and discussion

3.1 Characterization of jackfruit-derived cellulose nanocrystals (JCNCs)

The morphological and structural characteristics of cellulose nanocrystals derived from jackfruit (JCNCs) were thoroughly examined using TEM, SEM, XRD, and DLS techniques (Fig. 1). The TEM image (Fig. 1a) showed that the CNCs have a spherical

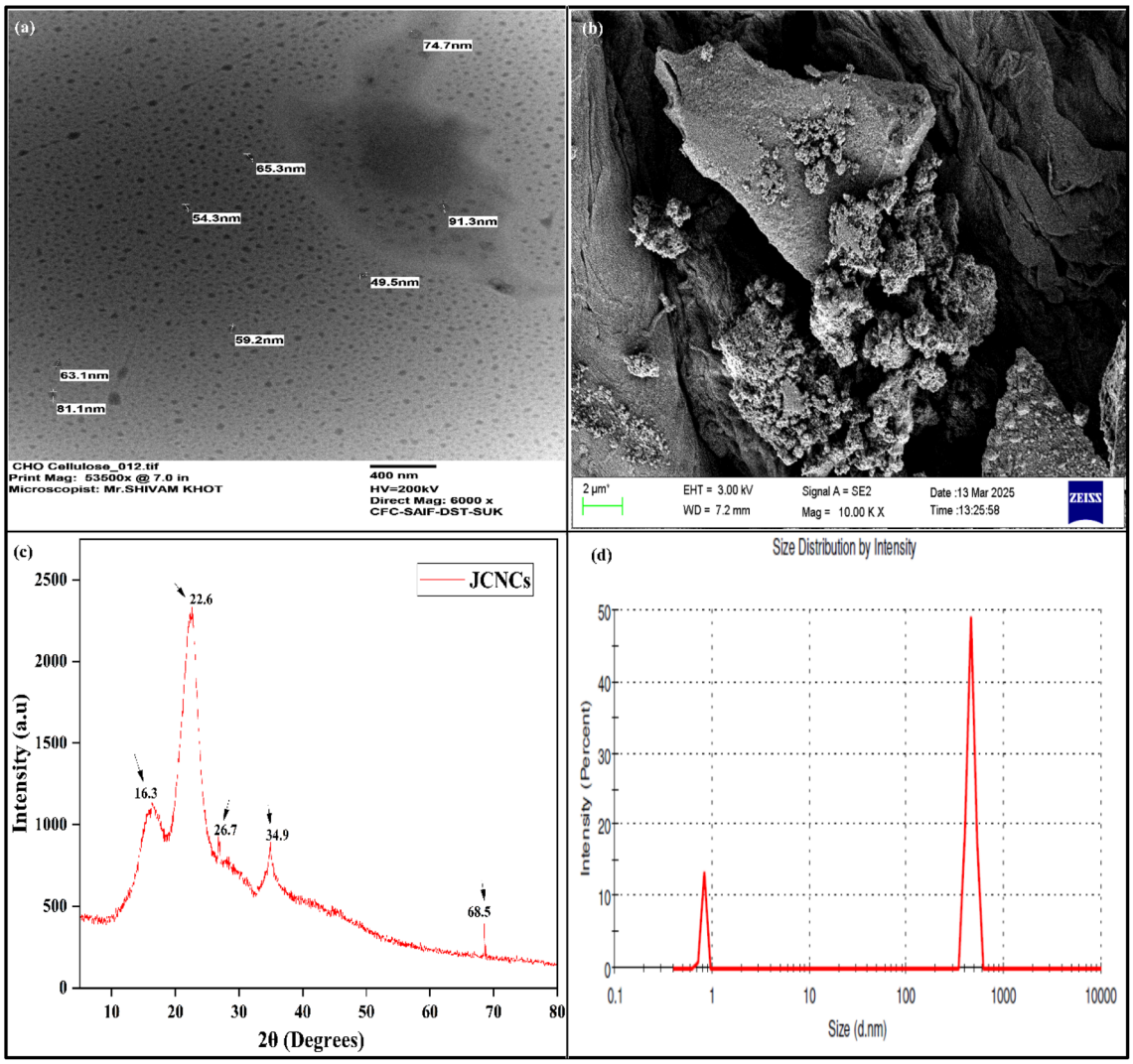

Fig. 1 (a) TEM image, (b) SEM micrograph, (c) XRD pattern, and (d) DLS profile of jackfruit-derived cellulose nanocrystals (JCNCs).

shape with particle sizes between 31.1 and 91.3 nm, which are ideal active agents for polymer matrices in food packaging. The nanoscale uniformity in the TEM image suggests effective acid hydrolysis, essential for achieving consistent barrier and mechanical properties. SEM analysis (Fig. 1b) revealed aggregated surface morphologies due to strong hydrogen bonding among hydroxyl-rich nanocrystals, a functional property that can enhance interfacial interactions when integrated into biopolymers, thus improving film integrity and reducing permeability. XRD analysis (Fig. 1c) confirmed the crystalline cellulose structure, with a sharp diffraction peak at $2\theta = 22.6°$ corresponding to the (200) plane, along with additional peaks at 16.3°, 26.7°, and 34.9°. The Segal empirical method was used to calculate the crystallinity index of the JCNCs, which was found to be high (69.9%). The relatively high crystallinity indicates efficient removal of amorphous components like hemicellulose and lignin, ensuring superior stiffness and transparency in packaging films. DLS analysis (Fig. 1d) further supported the nanoscale size distribution, with a dominant peak in the nanometre range, while a minor peak suggested limited aggregation in the aqueous suspension. These nanoscale dimensions, combined with high crystallinity, make JCNCs excellent candidates for active food packaging, where they can enhance mechanical strength, reduce oxygen and moisture permeability, and serve as carriers for bioactive compounds. Overall, these findings establish jackfruit waste-derived CNCs as sustainable, high-performance nanomaterials with significant potential in developing active and intelligent food packaging systems.

3.2 Fourier transform infrared (FTIR) spectroscopic analysis

To examine the chemical structure and possible intermolecular interactions within the films, the FTIR spectra of the control GK film and JCNC-reinforced films were analyzed (Fig. 2a). The FTIR spectrum of the control GK film displayed characteristic absorption bands of the gelatin/kappa-carrageenan matrix. The broad band in the 3300–3400 cm^{-1} region corresponds to overlapping –OH and –NH stretching vibrations arising from

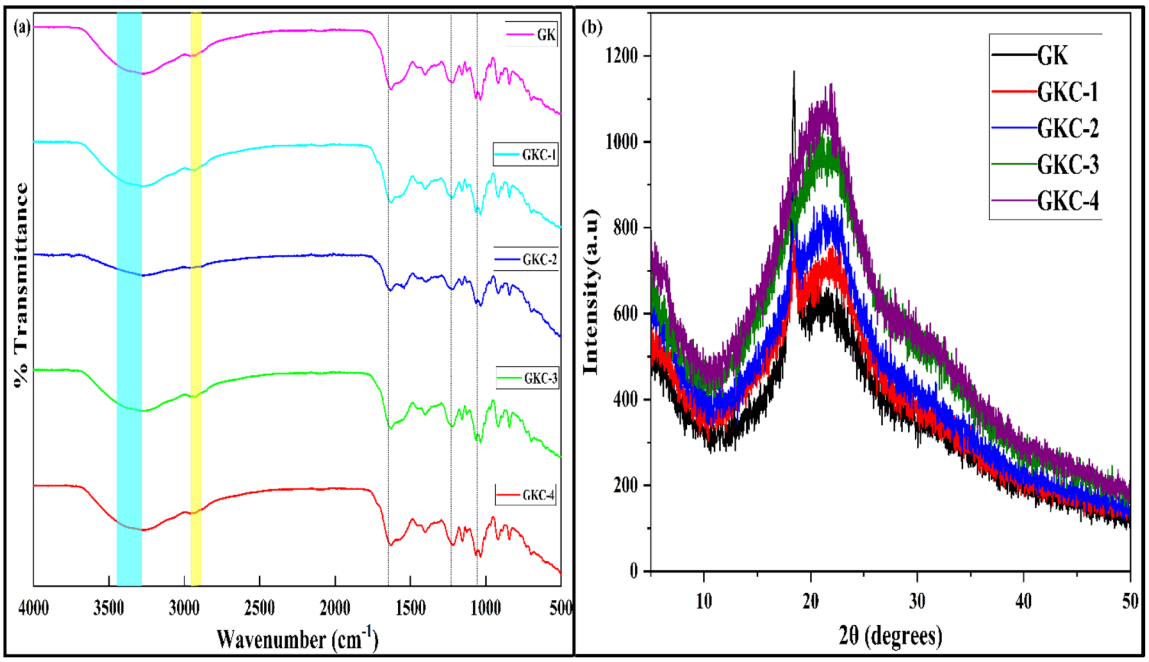

Fig. 2 (a) Fourier transformation infrared spectrograms. (b) X-ray diffractograms of prepared biopolymer films.

hydroxyl groups in kappa-carrageenan and amine groups in gelatin.[22] The peak observed at 1240 cm^{-1} is assigned to the S═O stretching vibration of sulfate groups present in kappa-carrageenan, while the amide I (≈1630 cm^{-1}, C═O stretching) and amide II (≈1530 cm^{-1}, N–H bending) bands are characteristic of the gelatin component.

Upon incorporation of JCNCs, no new absorption bands were observed, and the overall spectral profiles remained largely similar, indicating that the fundamental chemical structure of the polymer matrix was preserved. However, subtle changes in peak intensity and band broadening were noted. In particular, the broad –OH/–NH band in the 3300–3400 cm^{-1} region became more intense and slightly broader with increasing JCNC content, which can primarily be attributed to the introduction of hydroxyl-rich JCNCs rather than serving as direct evidence of newly formed hydrogen bonds. Similarly, the intensities of the C–O (≈1058 cm^{-1}) and C–O–C (≈1163 cm^{-1}) stretching bands increased gradually, reflecting the higher cellulose content in the composite films.[46] The amide I and II bands remained at similar wavenumbers after JCNC incorporation, suggesting that the gelatin secondary structure was largely retained. Minor intensity variations in these regions may indicate secondary intermolecular interactions between the matrix components and JCNCs, although FTIR alone cannot conclusively confirm specific hydrogen-bonding mechanisms. A slight change in the intensity of the sulfate group band at 1240 cm^{-1} was also observed, which may be associated with altered local environments of kappa-carrageenan chains in the presence of JCNCs.[19]

Additionally, enhanced absorption in the 2800–3000 cm^{-1} region (-CH stretching vibrations) was observed with increasing JCNC loading, consistent with the higher organic content of the films. Overall, the FTIR results suggest physical incorporation and molecular-level compatibility of JCNCs within the gelatin/kappa-carrageenan matrix, while structural and dispersion-related effects are more reliably supported by complementary SEM, XRD, and property analyses rather than FTIR alone.

3.3 X-ray diffraction (XRD) analysis

The XRD pattern of the control GK film exhibited a broad peak at 20° (101), signifying the semi-crystalline nature of GL, along with a smaller diffraction peak at 10° (002), which corresponds to the crystalline regions of KC[47] (Fig. 2b). The calculated crystallinity index of the control film (35%) aligns with the inherent semi-crystalline characteristics of GL and KC. However, upon incorporation of JCNCs, the XRD patterns of the composite films exhibited notable structural modifications. As the JCNC concentration increased, the diffraction peaks shifted to higher angles, reflecting enhanced molecular ordering within the polymeric matrix.[47] Specifically, the broad 20° (101) peak merged with the 23.0° (200) peak of JCNCs, resulting in a shift to 22.75°, while the 10° (002) peak of the control film migrated to 12.05° in GKC-4. These peak shifts suggest increased lattice spacing and improved structural organization due to the presence of JCNCs. The crystallinity index of the composite films progressively increased with JCNC incorporation, reaching 38% for GKC-1 (1% JCNC), 42% for GKC-2 (3% JCNC), 46% for GKC-3 (5% JCNC), and 49% for GKC-4 (7% JCNC). This trend confirms that JCNCs significantly enhance the crystalline nature of the films, owing to their rigid and highly ordered structural framework. Additionally, the sharpness and intensified intensity of the 15.6° (101), 23.0° (200), and 34.6° (400) peaks in the JCNC reinforced films further substantiate the strong intermolecular interactions between JCNCs and the biopolymeric matrix. These interactions primarily arise from hydrogen

bonding between the hydroxyl groups of JCNCs and the functional groups present in GK, leading to a denser and more structured film architecture. The increase in the crystallinity index of the composite films is mainly attributed to the incorporation of inherently highly crystalline JCNCs into the polymer matrix, rather than significant recrystallization of the gelatin/kappa-carrageenan network. Any contribution from improved chain packing is therefore considered secondary and limited. These findings are consistent with previous studies demonstrating that nanocellulose incorporation into biopolymeric matrices enhances crystallinity and overall film performance.[48,49]

3.4 Morphological analysis of biopolymeric films

The surface morphology and structural characteristics of GK films incorporated with varying concentrations of JCNCs were investigated using scanning electron microscopy (SEM). The SEM micrographs (Fig. 3) provided qualitative insights into the microstructural changes induced by JCNC incorporation, particularly at the local (microscale) level. The control film (GK) exhibited a relatively smooth and homogeneous surface with minor imperfections, which is typical of hydrophilic biopolymer-based films.[50] However, due to the inherent hydrophilic nature of gelatin (GL) and kappa-carrageenan (KC), partial solvent retention and uneven evaporation during film drying led to the formation of microvoids, resulting in a certain degree of surface porosity that may influence barrier properties.[51,52] In hydrophilic biopolymer systems such as gelatin and κ-carrageenan, the high density of polar functional groups (–OH, $–NH_2$, and $–SO_3^-$) promotes strong interactions with water during film casting, leading to uneven solvent evaporation and the formation of localized water-rich domains. Upon drying, these domains can generate microvoids or pores within the matrix, contributing to surface porosity, as commonly reported for hydrophilic biopolymer films.[51] The incorporation of JCNCs reduces this effect by filling interstitial spaces and reinforcing the polymer network, resulting in a denser and more compact film structure.[52]

Upon incorporation of JCNCs, notable changes in the film's surface morphology were observed. At 1% JCNC (GKC-1), the film exhibited a flat surface with dispersed JCNC particles. While minor agglomerations were evident, which is typical at lower nanofiller concentrations, the particles were well distributed within the matrix. As the JCNC concentration increased to 3% (GKC-2), the film surface became denser and more uniform, with a marked reduction in porosity.[53] This suggested that JCNCs effectively filled the interstitial spaces within the polymer network, thereby enhancing film integrity and compactness. At 5% JCNC (GKC-3), the film displayed a highly dense and homogeneous structure, with well-dispersed JCNC particles and further reduction in porosity. This microstructural improvement indicated strong interfacial interactions between JCNCs and the GK polymeric network, leading to the formation of a more cohesive and rigid structure. At the highest loading of 7% (GKC-4), the film exhibited locally compact regions; however, at larger length scales, the surface showed non-uniform, fiber-like or bundled domains. These features are attributed to partial self-association of JCNCs during solvent evaporation, driven by strong hydrogen bonding, rather than changes in the intrinsic nanoscale morphology of individual nanocrystals.

This evidence reveals localized aggregation and occasional larger JCNC domains, particularly at higher loadings, which can

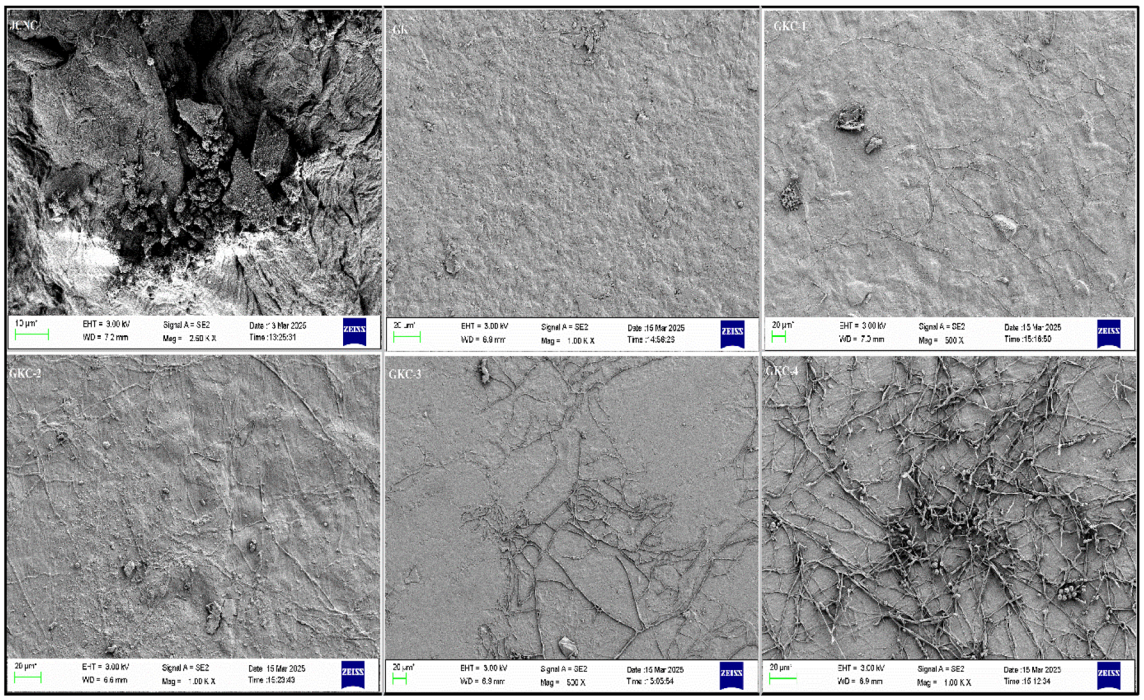

Fig. 3 The morphological results of JCNC, GK, GKC-1, GKC-2, GKC-3 and GKC-4 biopolymeric films.

be attributed to strong hydrogen-bonding interactions during film formation. These microstructural features correlate with the reduced visible light transmittance and enhanced UV-A and UV-B blocking, as increased light scattering and absorption contribute positively to the UV-barrier performance of the films.

3.5 Mechanical properties of biopolymeric films

The analysis reveals a steady rise in tensile strength as the concentration of JCNCs increases from GK to GKC-4 (Fig. 4a). The control sample (GK) exhibited the lowest tensile strength at 25.4 MPa, while the highest was recorded for GKC-4 at 72.1 MPa (Table 1). Conversely, elongation at break showed a marked decrease with the addition of JCNCs, particularly in GKC-4 (6.5%), indicating diminished flexibility. Young's modulus displayed a significant upward trend, indicating a notable increase in stiffness, especially for GKC-4 (3031.0 MPa), suggesting greater rigidity. This highlights the potential of JCNCs to enhance the mechanical properties of gelatin/κ-carrageenan films, albeit with a reduction in ductility. This trend aligns with previous reports on cellulose nanocrystal-incorporating films. Yadav *et al.* reported an increased tensile strength of 40% when cellulose nanocrystals were incorporated in alginate.[54] Similarly, Roy *et al.* reported that adding 5 wt% of CNC derived from onion peel extract to CMC/agar-based films increased strength by 25% and reduced flexibility by 60%.[55,56] The notable enhancement in the mechanical strength of the films can be primarily attributed to the reinforcing effect of JCNCs, which likely stems from strong hydrogen bonding interactions between the JCNCs and the control matrix (GK).[56] This improvement in mechanical performance is mainly due to the robust interfacial adhesion between the polymer matrix and JCNCs, along with the inherent rigidity and stiffness of the JCNCs (Table 4).[56]

3.6 Transparency and UV-blocking abilities of biopolymeric films

It is well known that UV irradiation accelerates the deterioration of packaged food; therefore, evaluating the UV-visible light response of the developed films is essential. Fig. 4b presents the UV-vis spectra of the prepared biopolymeric films. The transmittance at 280 nm (T_{280}) decreased markedly from 7.37% for the GK film to 0.57% for GKC-4, indicating a progressive reduction in UV transmittance with increasing JCNC content (Table 2). Similarly, the transmittance at 600 nm (T_{600}), which reflects overall visible transparency, decreased from 45.40% (GK) to 22.32% (GKC-4). Although increased matrix density typically improves transparency in homogeneous polymer systems, the reduction in visible light transmittance observed here cannot be attributed solely to decreased porosity. SEM analysis reveals the formation of larger, fibre-like or bundled JCNC-rich domains at higher loadings, which introduce refractive index heterogeneity and enhance light scattering, thereby reducing visible transparency. Consequently, the enhanced UV-blocking performance arises mainly from increased light absorption and scattering associated with these mesoscale structural features rather than porosity effects alone.[57–61]

Despite the reduction in transparency, the films retain sufficient visibility, making them suitable for food packaging applications where partial transparency is acceptable. Notably, the UV-A blocking efficiency increased from 73.66% (GK) to 92.01% (GKC-4), demonstrating the effectiveness of JCNCs in limiting longer-wavelength UV penetration. Likewise, the UV-B blocking capacity improved from 87.1% to 97.76%, providing critical protection against more harmful short-wavelength UV radiation. While high transparency is preferred for certain packaging applications, controlled opacity combined with strong UV shielding is advantageous for light-sensitive foods to

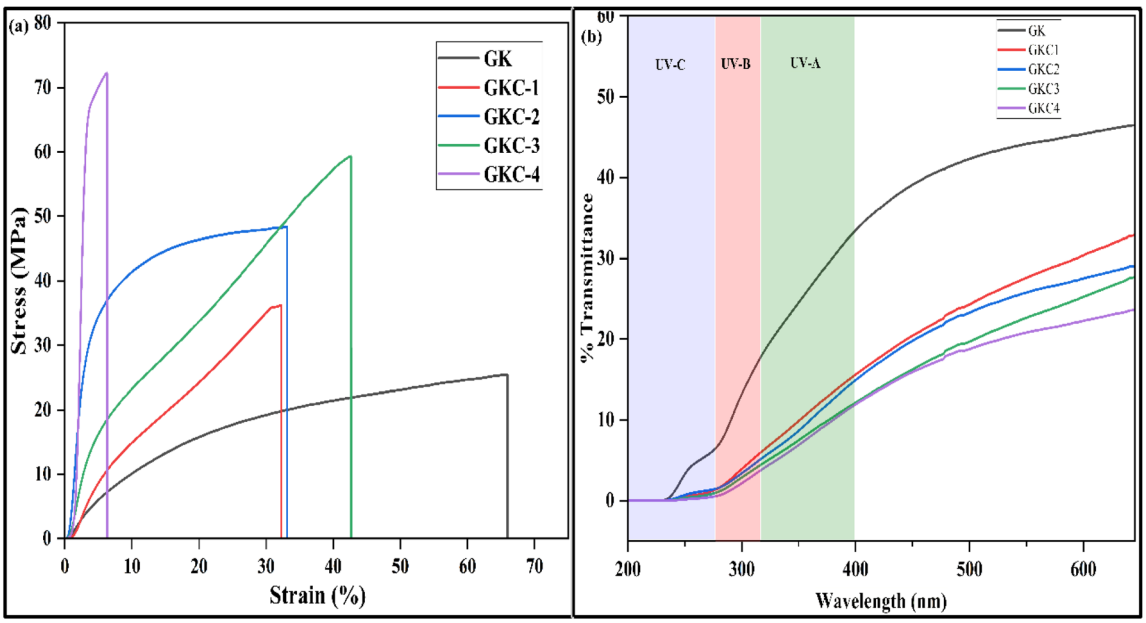

Fig. 4 (a) Stress *vs.* strain curves. (b) UV-vis spectrograms of prepared biopolymeric films.

Table 1 Thickness, tensile strength, elongation at break and Young's modulus of biopolymeric films

Films	Thickness (mm)	Tensile strength (MPa)	Elongation at break (%)	Young's modulus (MPa)
GK	0.05 ± 0.2^{a}	25.4 ± 1.08^{b}	74.8 ± 0.60^{a}	150.5 ± 0.87^{a}
GKC-1	0.06 ± 0.15^{b}	36.2 ± 1.09^{a}	33.9 ± 0.48^{b}	255.4 ± 0.80^{b}
GKC-2	0.06 ± 0.12^{b}	48.3 ± 1.01^{c}	52.3 ± 0.37^{c}	1131.8 ± 0.63^{d}
GKC-3	0.07 ± 0.08^{c}	59.3 ± 0.88^{d}	42.9 ± 0.25^{d}	472.3 ± 0.68^{c}
GKC-4	0.07 ± 0.04^{d}	72.1 ± 0.68^{e}	6.5 ± 0.24^{d}	3031.0 ± 0.57^{e}

Table 2 % Transmittance at 280 & 600 nm and UV blocking % of prepared films

Films	T_{280} (%)	T_{600} (%)	UV-A blocking (%)	UV-B blocking (%)
GK	7.3 ± 0.2^{a}	45.4 ± 1.8^{a}	73.6 ± 0.2^{a}	87.1 ± 0.9^{a}
GKC-1	1.6 ± 0.1^{b}	30.4 ± 1.2^{b}	88.9 ± 0.1^{b}	96.05 ± 0.0^{b}
GKC-2	1.6 ± 0.1^{b}	27.4 ± 1.1^{c}	89.9 ± 0.06^{c}	96.5 ± 0.4^{b}
GKC-3	1.1 ± 0.08^{c}	25.1 ± 0.9^{d}	91.5 ± 0.07^{c}	97.1 ± 0.4^{c}
GKC-4	0.5 ± 0.05^{d}	22.3 ± 0.8^{e}	92.0 ± 0.1^{d}	97.7 ± 0.2^{d}

mitigate photo-oxidation and quality degradation. Moreover, JCNCs are incorporated not merely as UV-blocking agents but as multifunctional reinforcements that simultaneously enhance mechanical strength, barrier performance, antioxidant activity, and overall sustainability of the packaging films.

3.7 Water vapour permeability of prepared biopolymeric films

As the concentration of JCNCs in the films increased, the WVP values showed a consistent decline (Table 3). The control film (GK) demonstrated the highest WVP value at 5.18×10^{-7} g h^{-1} m^{-1} Pa^{-1}, suggesting a greater transmission of water vapour. With the rise in JCNC content from 1% to 7%, the WVP values notably decreased, with GKC-4 exhibiting the lowest WVP value of 3.60×10^{-7} g h^{-1} m^{-1} Pa^{-1}. This observed decrease in WVP can be explained by the addition of JCNCs, which establishes a more complex pathway for water vapour diffusion.[49] This occurs due to the formation of a compact and interlinked network within the polymer matrix. Y. He *et al.*'s earlier research, which showed that incorporating JCNC-based nanocomposites into polymer matrices successfully decreased water vapour permeability, is consistent with the study's WVP decrease.[62] This decrease is mostly explained by the formation of a more intricate water molecule diffusion pathway, which lengthens the effective path and greatly improves the barrier qualities of the film. Cellulose nanocrystals are amphiphilic in nature but remain predominantly hydrophilic rather than inherently hydrophobic, as widely reported in the literature. Accordingly, the observed increase in the water contact angle is attributed not solely to the surface chemistry of JCNCs, but to the combined effect of JCNC incorporation and the resulting changes in surface morphology and roughness of the films, as evidenced by SEM analysis.

3.8 Oxygen transmission rate of biopolymeric films

A steady decrease in OTR values was observed as the JCNC content in the films increased (Table 3). The GK control film showed the highest OTR value of 1.508 g h^{-1} m^{-1} atm^{-1}, suggesting greater oxygen permeability. As the JCNC concentration rose from 1% to 7%, OTR values significantly dropped, with GKC-4 recording the lowest at 0.612 h^{-1} m^{-1} atm^{-1}. This OTR reduction can be linked to CNC incorporation, which creates a strong interface between JCNCs and the GK matrix, further limiting oxygen movement and enhancing film barrier properties. The continuous OTR decline with increasing JCNC content highlights JCNC's role as a reinforcing agent in improving the oxygen barrier properties of biopolymer films. This trend is consistent with that in previous research reporting similar barrier performance improvements when nanocellulose is added to polymer matrices. Y. He *et al.* reported that adding JCNC-based nanocomposites to a coating matrix successfully reduced air permeability, which is consistent with the improved oxygen barrier performance in this investigation.[62] The capacity of JCNCs to fill in spaces between polymer chains and create

Table 3 Results of water vapour permeability, oxygen transmission rate, water solubility, moisture retention capacity and soil burial test of prepared biopolymeric films

Sample code	WVP ($\times 10^{-7}$ g h^{-1} m^{-1} Pa^{-1})	OTR ($\times 10^{-6}$ g h^{-1} m^{-1} atm^{-1})	WS (%)	MRC (%)	Soil burial test (%)
GK	5.1 ± 0.1^{a}	1.5 ± 0.03^{a}	9.5 ± 0.2^{a}	9.8 ± 0.1^{a}	42.1 ± 0.8^{a}
GKC-1	5.01 ± 0.1^{ab}	1.2 ± 0.04^{b}	9.1 ± 0.1^{a}	9.6 ± 0.1^{ab}	38.5 ± 1.1^{ab}
GKC-2	4.7 ± 0.09^{bc}	0.9 ± 0.02^{c}	8.5 ± 0.2^{b}	9.1 ± 0.1^{b}	34.2 ± 0.7^{b}
GKC-3	4.2 ± 0.08^{cd}	0.7 ± 0.01^{d}	8.1 ± 0.2^{bc}	8.8 ± 0.1^{bc}	29.1 ± 0.9^{c}
GKC-4	3.6 ± 0.07^{d}	0.6 ± 0.02^{d}	7.9 ± 0.2^{c}	8.7 ± 0.1^{d}	25.6 ± 0.1^{d}

a highly ordered "nano-brick" structure was linked to this improvement. Consequently, the oxygen diffusion pathway's increased tortuosity helped improve the barrier's overall qualities.

3.9 Water solubility of biopolymeric films

Incorporating JCNCs into the GK matrix significantly influenced the composite films' water solubility (WS). The GK control film exhibited the highest WS value of 9.512%, highlighting the inherently hydrophilic nature of GL and KC.[63] However, as the JCNC concentration increased from 1% to 7%, WS values steadily declined, with the GKC-4 film displaying the lowest WS value of 7.924% (Table 3). This reduction in WS can be attributed to the formation of strong intermolecular hydrogen bonds between JCNCs and the GK polymer network, which restricts the penetration of water molecules into the film matrix.[64] Additionally, JCNCs enhance film structural integrity through cross-linking interactions, reinforcing the polymeric network and making it more resistant to dissolution. The hydrophobic nature of JCNCs further decreases water affinity, thereby improving the overall water resistance of the films.

3.10 Moisture retention capacity of biopolymeric films

MRC values showed a gradual decrease with increasing CNC content in the films (Table 3). The GK control film demonstrated the highest MRC value of 9.899%, indicating greater moisture retention. As the JCNC concentration rose from 1% to 7%, MRC values decreased, with GKC-4 recording the lowest MRC value of 8.781%. This MRC reduction can be attributed to JCNC incorporation, which decreases overall film hydrophilicity by forming a more compact and cross-linked network. The JCNCs' presence restricts moisture absorption and retention within the polymer matrix, thus lowering the MRC.[65]

3.11 Soil burial test of the prepared biopolymeric films

The biopolymeric films exhibit inherent biodegradability due to their natural polymer backbone and hydrolysable functional groups, enabling degradation through hydrolytic, enzymatic, and microbial pathways in soil or compost environments. Moisture-assisted chain scission and subsequent microbial mineralization govern the degradation process, which is influenced by the polymer structure and composition. Consistent with recent studies, the developed films are expected to balance functional performance with environmentally favorable degradation behavior, supporting their application in sustainable packaging.[66,67] The biodegradability of the fabricated nanocomposite films was evaluated through a soil burial test, wherein the films were buried in soil for 30 days, with periodic monitoring of their weight loss and physical degradation. The control GK film exhibited a 42.1% weight reduction by the end of the study, indicating a moderate degree of biodegradability (Table 3). In contrast, films containing jackfruit cellulose nanocrystals (JCNCs) demonstrated varied degradation rates, with weight loss values ranging from 38.5% to 25.6% over the same period. Specifically, the weight reduction for GKC-1, GKC-2, GKC-3 and GKC-4 was recorded as 38.5%, 34.2%, 29.1% and 25.6%, respectively. Visual assessments further substantiated these findings. By 20 days, the control GK film exhibited visible cracks and substantial disintegration, signifying extensive microbial degradation. Conversely, JCNC incorporating films displayed a more intact structure, with GKC-4 showing the least fragmentation and cracking even after 30 days. These observations suggest that CNC incorporation reduces the rate of biodegradation in GK films.

The reduced biodegradability of JCNC reinforced films can be attributed to increased hydrophobicity, which hinders microbial colonization and enzymatic breakdown. As CNC content increases, the films develop a more compact and water-resistant structure, thereby limiting microbial access to degradable sites. This trend aligns with previous studies, which report that CNCs enhance the mechanical strength and thermal stability of biopolymeric films, consequently reducing their susceptibility to microbial degradation.[68] Additionally, CNCs may act as a physical barrier, restricting the exposure of the film's surface to enzymes and microbial activity, further slowing

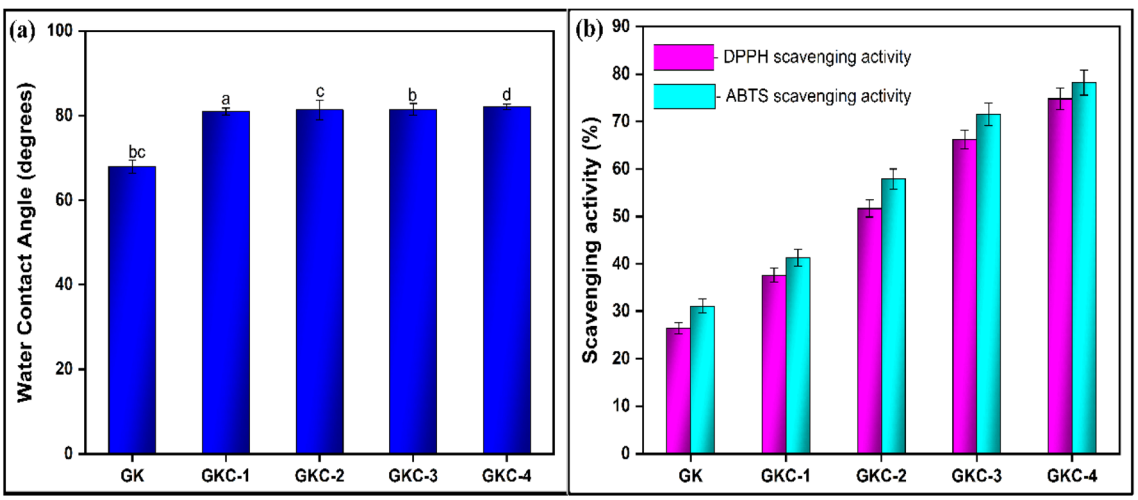

Fig. 5 (a) The water contact angles and (b) DPPH and ABTS scavenging activities of the fabricated biopolymeric films.

down the degradation process. These findings hold significant implications for the development of biodegradable packaging materials. While the incorporation of JCNCs enhances the structural and thermal properties of GK films, it simultaneously reduces their biodegradation rate. Therefore, balancing mechanical durability and environmental sustainability remains a critical factor in optimizing CNC-based biodegradable films for eco-friendly packaging applications.

The soil burial test employed in this study provides a qualitative and comparative indication of environmental disintegration rather than a definitive measure of intrinsic biodegradation, particularly for hydrophilic and partially water-soluble polymers such as gelatin and kappa-carrageenan. Under soil conditions, the observed mass loss may arise from a combination of microbial degradation and moisture-induced dissolution; however, the test remains useful for comparing relative stability and degradation trends among films with different JCNC loadings under identical conditions.

3.12 Wettability of the prepared biopolymeric films

The addition of JCNCs to GK films resulted in notable changes to the composite films' water contact angle (WCA). The baseline film exhibited a WCA of 67.9° (Fig. 5a), suggesting a somewhat hydrophilic surface, as noted by Paula *et al.*[69] As JCNC concentrations increased, a gradual rise in the WCA was noted. The highest WCA of 82.1° was observed in the film with 7% JCNCs.[70] Films GKC-1, GKC-2 and GKC-3 showed WCAs of 81.0°, 81.4° and 81.5°, respectively.[71] As explained by Kono *et al.*, the rise in the WCA following JCNC incorporation can be linked to the naturally hydrophobic nature of cellulose nanocrystals.[72] The introduction of JCNCs into the GK matrix likely interrupts the continuity of the hydrophilic polymer network, creating a more heterogeneous surface with decreased wettability.[73] This observation is consistent with previous research by Achaby *et al.*, which has documented comparable increases in the WCA for polymer composites strengthened with hydrophobic nanofillers.[74]

3.13 Antioxidant properties of the fabricated biopolymeric films

The antioxidant potential of GK composite films incorporating varying concentrations of JCNCs was systematically evaluated using DPPH and ABTS radical scavenging assays (Fig. 5b). The control film exhibited inherent but limited radical-scavenging activity, with baseline values of 26.5 ± 1.2% for DPPH and 31.1 ± 1.5% for ABTS, highlighting the intrinsic antioxidant capacity of the GK matrix.[75] The incorporation of 1% JCNCs into the GK matrix resulted in a significant enhancement, with antioxidant activity increasing to 37.6 ± 1.5% (DPPH) and 41.3 ± 1.8% (ABTS). A clear concentration-dependent trend was observed, with GKC-2 exhibiting 51.7 ± 1.8% (DPPH) and 57.9 ± 2.1% (ABTS) and GKC-3 further improving to 66.2 ± 2.0% (DPPH) and 71.5 ± 2.4% (ABTS). Notably, GKC-4 demonstrated the highest antioxidant efficacy, reaching 74.8 ± 2.3% (DPPH) and 78.2 ± 2.6% (ABTS), nearly threefold that of the control. This progressive enhancement in antioxidant activity can be

Table 4 Comparative properties of cellulose nanocrystal (CNC) incorporating films/composites

Composite material	CNC content	Tensile strength (TS)/mechanical properties	UV-blocking ability	Antioxidant & antimicrobial activity	Reference
Chitosan/CNC	0–50 wt%	TS increased: 7.98 MPa (neat) and 25.3 MPa (50 wt% CNC). Young's modulus: 22.4 MPa to 92.7 MPa (50 wt% CNC)	Transparency: decreased as CNC content increased (transparency value is 0.75–1.0)	Antimicrobial: "Total" inhibition against *S. aureus*, *E. coli*, and *C. albicans* at 10–25 wt% CNC	78
Chitosan/CNC	4 wt%	TS increased: improved by 39% compared to neat chitosan. Young's modulus: improved by 78%	Improved: UV barrier properties demonstrated better performance than those of neat chitosan films	—	79
Chitosan/anthocyanin/CNC	Not specified	TS increased: 15 MPa to 35 MPa	UV blocking: 0% UV transmittance (high blocking) reported	Antioxidant & antimicrobial: increased properties; used for shrimp preservation and freshness monitoring	80
Natural rubber/CNC (from pine)	1–5 wt%	TS increased: Tensile strength, tensile modulus, and storage modulus increased	—	—	81
Present work	1–7 wt%	TS increased: 25.4 MPa to 72.1 MPa (GKC-4). Young's modulus was also improved	UV blocking: 73.66% for the control film to 92.01% for the 7% CNC containing film (GKC-4)	Antioxidant: 74.8% for DPPH and 78.2% for ABTS for the 7% CNC containing film (GKC-4)	—

attributed to multiple factors, including the high density of hydroxyl functional groups in JCNCs,[76] which serve as effective hydrogen donors, improved structural integrity that mitigates oxidative degradation, and potential synergistic interactions between JCNCs and the biopolymer matrix.[77] The antioxidant activity observed in JCNC-containing films cannot be attributed solely to the aliphatic hydroxyl groups of cellulose, which are inherently weak radical scavengers. Instead, this activity is more plausibly associated with trace residual phenolic compounds or other bioactive constituents originating from jackfruit peel biomass that may persist after purification, along with their synergistic interactions within the biopolymer matrix.

3.14 Packaging studies

Button mushrooms (*Agaricus bisporus*) were chosen for packaging studies because they are one of the most widely cultivated and consumed mushroom varieties globally, with high commercial importance. Their delicate texture, high moisture content, and rapid post-harvest respiration rate make them particularly prone to quality deterioration and spoilage, necessitating effective packaging to retain freshness, extend shelf life and reduce losses during storage and transportation.

3.15 pH variation and weight loss studies

The quality of button mushrooms stored at 4 °C was evaluated over 12 days by analyzing two primary factors: weight loss (%) and pH changes, under four distinct packaging conditions: unpacked, GK (control film), GKC-4 and commercial polyethene film (Fig. 6).

Across all packaging systems, button mushrooms showed progressive quality changes during storage, with packaging markedly moderating both acidification and moisture loss. The initial pH was identical (6.86) for all treatments, confirming comparable starting conditions (Fig. 7a). Thereafter, unpacked mushrooms acidified rapidly to 5.90 ± 0.23 (day 3), 5.42 ± 0.25 (day 6), 5.25 ± 0.27 (day 9), and 4.04 ± 0.24 (day 12; $\Delta pH = -2.82$), indicative of intensified respiration and microbial activity. Packaging mitigated this shift, with the control film

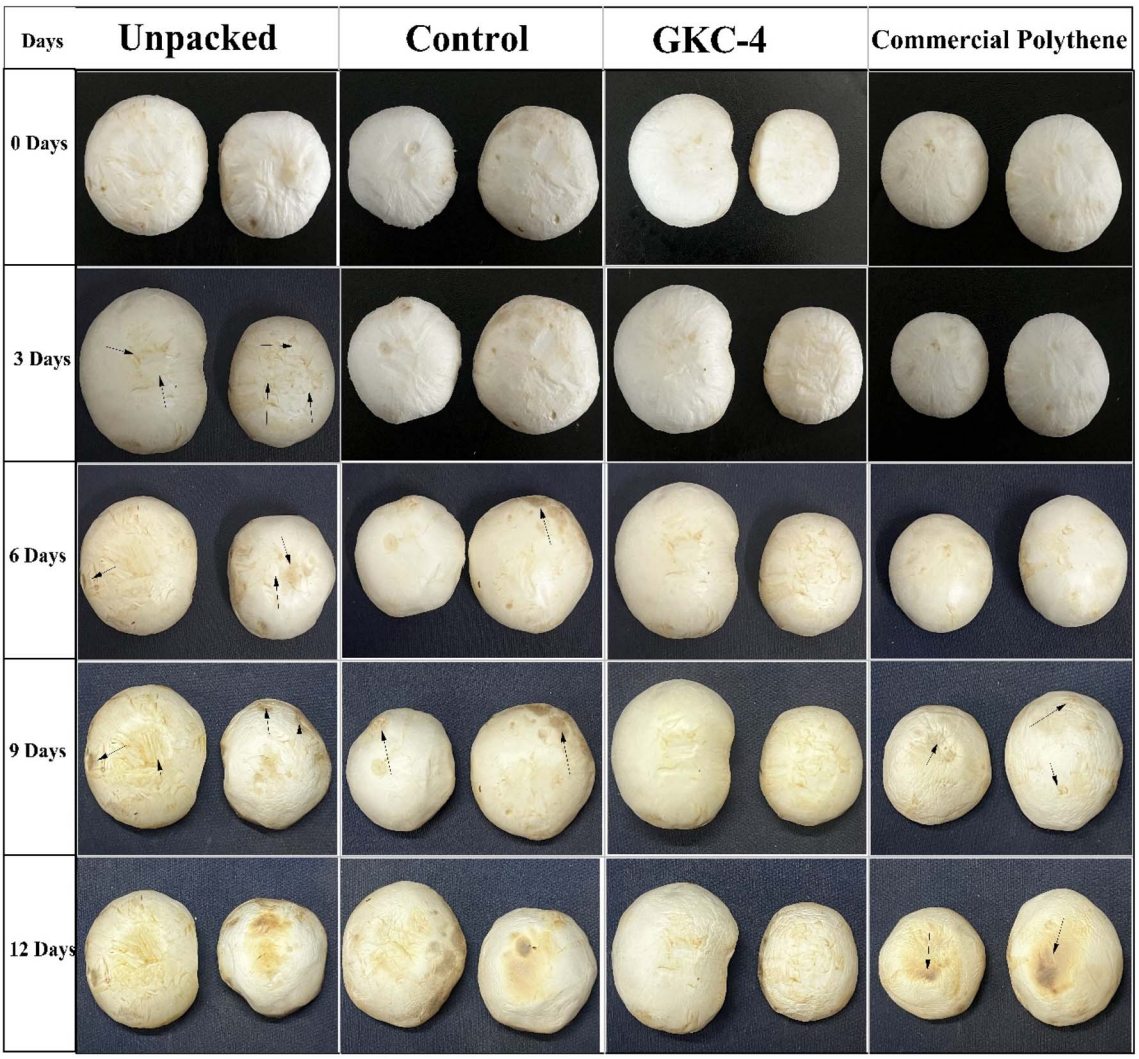

Fig. 6 Visual appearance of button mushrooms unpacked and packed with control, GKC-4 and polythene films.

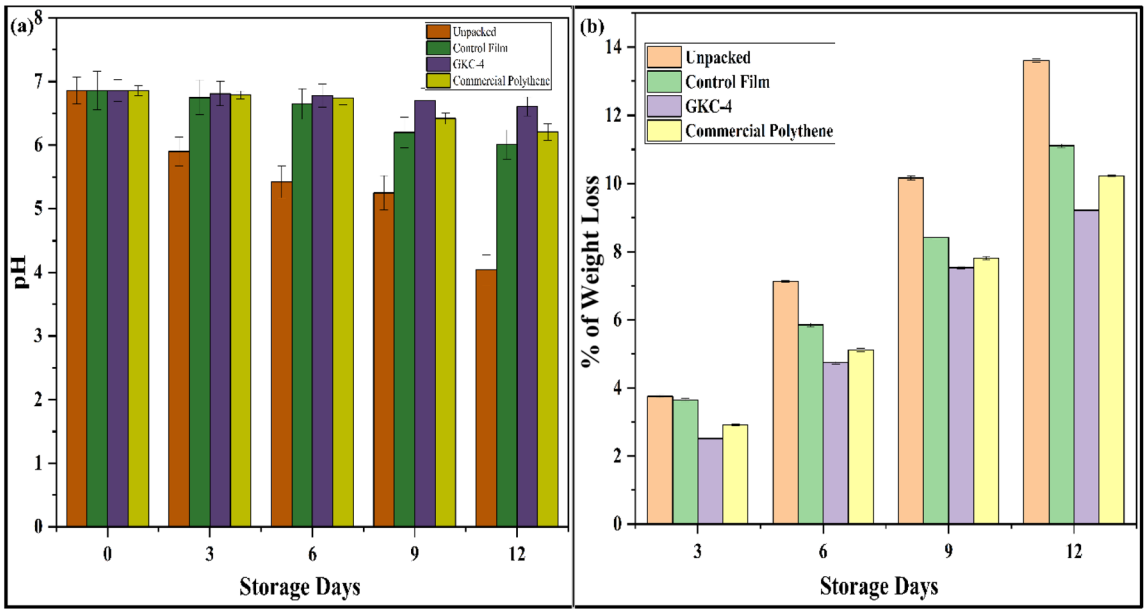

Fig. 7 (a) Observed variations in the pH and (b) weight % of the packed button mushrooms on the 0th, 3rd, 6th, 9th and 12th days, respectively.

declining to 6.01 ± 0.23 (ΔpH = −0.85), commercial polythene declining to 6.21 ± 0.13 (ΔpH = −0.65), and GKC-4 showing the greatest pH stability at 6.61 ± 0.15 by day 12 (ΔpH = −0.25). The treatment gaps at each time point (at day 12: 6.61 *vs.* 6.21 *vs.* 6.01 *vs.* 4.04) are much larger than their associated errors (±0.06–0.30), supporting the robustness of these differences.

Parallel trends were observed for cumulative weight loss (Fig. 7b). By day 3, unpacked samples lost 3.76 ± 0.05% compared to 3.65 ± 0.04% for the control film, 2.92 ± 0.03% for commercial polythene and 2.52 ± 0.02% for GKC-4. By day 6, the pattern widened to 7.13 ± 0.03% for unpacked, 5.85 ± 0.05% for the control film, 5.11 ± 0.05% for commercial polythene, and 4.74 ± 0.04% for GKC-4. Similarly, by day 12 the values were 13.61 ± 0.05%, 11.11 ± 0.05%, 10.22 ± 0.03%, and 9.21 ± 0.02%, respectively. Relative to unpacked mushrooms, GKC-4 reduced weight loss by about 33% on day 6 and 32% on day 12, with commercial polythene achieving ∼28% and ∼25% reductions and the control film achieving ∼18% reductions at these times; the small standard deviations (±0.02–0.06) indicate high measurement precision. Mechanistically, GKC-4 likely offers superior barrier and gas-modulating properties that limit transpiration and oxidative metabolism while suppressing microbial proliferation, thereby retaining near-neutral pH, reducing shrivelling, and sustaining texture and overall acceptability over the 12-day storage period.

3.16 Sensory results and interpretation

All samples started with very high quality on day 0 (approximately 9.3–9.6 out of 10 across attributes) and then declined during storage, with the rate of decline strongly dependent on

Table 5 The sensory results of various packaging systems

Sample	Attribute	Day 0	Day 3	Day 6	Day 9	Day 12
Unpacked	Appearance	9.6 ± 0.3	8.1 ± 0.6	6.3 ± 0.5	5.7 ± 0.7	4.2 ± 0.8
	Texture	9.4 ± 0.4	8.2 ± 0.6	6.2 ± 0.7	5.5 ± 0.7	4.0 ± 0.4
	Odor	9.3 ± 0.4	8.9 ± 0.6	5.7 ± 0.7	5.2 ± 0.9	3.7 ± 0.8
	Overall acceptability	9.5 ± 0.3	8.0 ± 0.5	6.1 ± 0.6	5.6 ± 0.5	4.1 ± 0.7
Polyethene film	Appearance	9.6 ± 0.3	8.9 ± 0.4	7.5 ± 0.5	7.0 ± 0.3	6.7 ± 0.8
	Texture	9.5 ± 0.3	8.7 ± 0.4	7.1 ± 0.5	6.8 ± 0.2	6.5 ± 0.9
	Odor	9.6 ± 0.3	8.5 ± 0.5	7.2 ± 0.5	6.7 ± 0.4	4.4 ± 0.9
	Overall acceptability	9.5 ± 0.2	8.6 ± 0.4	7.1 ± 0.4	6.8 ± 0.1	5.6 ± 0.8
GK film (control)	Appearance	9.6 ± 0.3	8.1 ± 0.4	7.5 ± 0.5	7.2 ± 0.4	6.9 ± 0.9
	Texture	9.5 ± 0.3	7.9 ± 0.4	7.4 ± 0.4	7.1 ± 0.4	6.7 ± 0.8
	Odor	9.4 ± 0.3	8.7 ± 0.5	7.2 ± 0.5	6.9 ± 0.3	5.6 ± 0.8
	Overall acceptability	9.5 ± 0.2	8.8 ± 0.3	7.2 ± 0.4	7.0 ± 0.2	6.7 ± 0.9
GKC-4 film	Appearance	9.6 ± 0.3	8.3 ± 0.3	8.2 ± 0.4	7.9 ± 0.3	7.7 ± 0.9
	Texture	9.5 ± 0.3	8.2 ± 0.3	8.1 ± 0.4	7.8 ± 0.4	7.6 ± 0.8
	Odor	9.5 ± 0.3	8.2 ± 0.3	8.2 ± 0.4	7.8 ± 0.3	7.6 ± 0.7
	Overall acceptability	9.3 ± 0.2	8.3 ± 0.3	8.2 ± 0.3	7.9 ± 0.2	7.7 ± 0.9

packaging type (Table 5). Unpacked samples deteriorated the fastest, falling by day 12 to 4.2 ± 0.8 for appearance, 4.0 ± 0.4 for texture, 3.7 ± 0.8 for odor, and 4.1 ± 0.7 for overall acceptability, indicating pronounced losses in visual quality, firmness, and aroma. The polyethene film mitigated these losses to an extent, retaining day-12 appearance and texture at 6.7 ± 0.8 and 6.5 ± 0.9, respectively, but odor dropped sharply to 4.4 ± 0.9, limiting overall acceptability to 5.6 ± 0.8. The GK film outperformed polyethene, with day-12 scores of 6.9 ± 0.9 for appearance, 6.7 ± 0.8 for texture, 5.6 ± 0.8 for odor and 6.7 ± 0.9 for overall acceptability, showing better preservation of aroma and consumer appeal. The GKC-4 film consistently provided better retention of sensory quality, remaining near or above 7.6 out of 10 for all attributes on day 12 (appearance at 7.7 ± 0.9, texture at 7.6 ± 0.8, odor at 7.6 ± 0.7, and overall acceptability at 7.7 ± 0.9). Notably, by day 6, the GKC-4 film still sustained scores around 8.1–8.2 while the scores of polyethene and GK films had dropped to approximately 7.1–7.4 and the unpacked sample dropped to 6.1 for overall acceptability. These results demonstrate that packaging markedly slows sensory quality loss relative to no packaging, with GKC-4 offering the strongest protection across appearance, texture, and odor, definitely due to superior barrier properties that limit moisture loss, oxidative changes, and aroma volatilization, thereby delivering better overall acceptability throughout the 12-day storage.

5 Conclusion

This study demonstrates that cellulose nanocrystals derived from jackfruit peel (JCNCs) are effective bio-based reinforcements for gelatin/kappa-carrageenan (GK) biopolymeric films, producing concurrent improvements in the structure, barrier performance, mechanics, and functionality. Among the formulations, GKC-4 emerged as the optimal film, exhibiting a 30.5% reduction in water vapor permeability and an 87% increase in tensile strength, alongside substantial gains in antioxidant capacity *i.e.*, DPPH (182.264%) and ABTS (151.447%) relative to the GK control. Soil burial tests indicated a 39.19% decrease in the degradation rate for GKC-4, suggesting an extended functional lifetime while retaining biodegradability. Packaging experiments were conducted with button mushrooms stored at 4 °C for 12 days. GKC-4 significantly outperformed the unpackaged control and commercial polyethene films, minimising weight loss to 9.21 ± 0.02% and retaining pH stability at 6.61 ± 0.15. These results verify that JCNC reinforcement can translate laboratory-scale property enhancements into tangible preservation benefits for perishable foods.

Overall, the valorization of jackfruit peel into JCNCs offers a sustainable pathway to high-performance, active biopolymer films. GKC-4, in particular, shows strong potential as a functional, biodegradable alternative to conventional plastics for food packaging. Although the JCNC-reinforced gelatin/kappa-carrageenan films exhibited improved functional and packaging performance, the study is limited to laboratory-scale fabrication, short-term storage, and a single food model. Future work should focus on scale-up feasibility, long-term storage studies under diverse environmental conditions, safety and migration assessments, and evaluation with different food systems to support practical and regulatory implementation of these films in real-world packaging applications.

Author contributions

Ajitkumar Appayya Hunashyal: conceptualization, data interpretation, formal analysis, writing – original draft. Saraswati P. Masti: supervision, corresponding author, review, and manuscript corrections. Lingaraj Kariyappa Kurabetta: data curation, formal analysis. Manjushree Nagaraj Gunaki: study design, formal analysis, data curation, investigation. Jennifer P Pinto: conceptualization, data interpretation, review. Priyadarshini: data curation, formal analysis. Shiddalingesh G. Havanur: resources, manuscript corrections. Bhagyalakshmi A. Sheeparamatti: resources, manuscript corrections. Priyanka Baburao: resources, manuscript corrections. Ravindra B. Chougale: manuscript correction.

Conflicts of interest

The authors declare no conflict of interest.

Data availability

The data supporting the findings of this study are available from the corresponding author upon reasonable request.

Acknowledgements

The authors are thankful to the Science and Engineering Research Board (SERB) for providing instrumental facilities under the project sanctioned to Dr Saraswati P. Masti, Principal Investigator, SERB (Sanction Letter No. SB/EMEQ-213/2014 dated: 29-01-2016). We gratefully acknowledge the Sophisticated Analytical Instrumentation Facilities (SAIF), University Scientific and Instrumentation Centre (USIC), and DST-PURSE Phase II Program [Grant No. SR/PURSE PHASE-2/13(G)], Karnatak University, Dharwad, for providing necessary instrumentation support. Mr Ajitkumar Appayya Hunashyal extends his gratitude to KSTePS, Karnataka, India, for awarding a K-DST Research Fellowship. The authors sincerely acknowledge Ms Pooja, Ms Usha, and Mr Kiran for their valuable technical assistance and support.

References

1 O. M. Atta, S. Manan, A. Shahzad, M. Ul-Islam, M. W. Ullah and G. Yang, Biobased materials for active food packaging: A review, *Food Hydrocoll.*, 2022, **125**, 107419.
2 Q. Wang, W. Chen, W. Zhu, D. J. McClements, X. Liu and F. Liu, A review of multilayer and composite films and coatings for active biodegradable packaging, *NPJ Sci Food*, 2022, **6**(1), 18.

3 M. Ghasemlou, C. J. Barrow and B. Adhikari, The future of bioplastics in food packaging: An industrial perspective, *Food Packag. Shelf Life*, 2024, **43**, 101279.
4 D. Winton, L. Marazzi and S. Loiselle, Drivers of public plastic (mis)use — New insights from changes in single-use plastic usage during the Covid-19 pandemic, *Sci. Total Environ.*, 2022, **849**, 157672.
5 S. A. Mir, B. N. Dar, A. A. Wani and M. A. Shah, Effect of plant extracts on the techno-functional properties of biodegradable packaging films, *Trends Food Sci. Technol.*, 2018, **80**, 141–154.
6 J. G. Rosenboom, R. Langer and G. Traverso, Bioplastics for a circular economy, *Nat. Rev. Mater.*, 2022, **7**(2), 117–137.
7 J. Lv, D. Zhang, X. Li, Y. Miao, Y. Wang, Y. Wang, *et al.*, Reversible biobased adhesives enable closed-loop engineered composites, *Nat. Commun.*, 2025, **16**(1), 7871.
8 C. Li, J. Liu, W. Li, Z. Liu, X. Yang, B. Liang, *et al.*, Biobased Intelligent Food-Packaging Materials with Sustained-Release Antibacterial and Real-Time Monitoring Ability, *ACS Appl. Mater. Interfaces*, 2023, **15**(31), 37966–37975.
9 S. Jafarzadeh, S. M. Jafari, A. Salehabadi, A. M. Nafchi, U. S. Uthaya Kumar and H. P. S. A. Khalil, Biodegradable green packaging with antimicrobial functions based on the bioactive compounds from tropical plants and their by-products, *Trends Food Sci. Technol.*, 2020, **100**, 262–277.
10 J. R. Westlake, M. W. Tran, Y. Jiang, X. Zhang, A. D. Burrows and M. Xie, Biodegradable biopolymers for active packaging: demand, development and directions, *Sustainable Food Technol.*, 2023, **1**(1), 50–72.
11 S. M. El-Sayed and A. M. Youssef, Eco-friendly biodegradable nanocomposite materials and their recent use in food packaging applications: a review, *Sustainable Food Technol.*, 2023, **1**(2), 215–227.
12 E. Tavassoli-Kafrani, M. V. Gamage, L. F. Dumée, L. Kong and S. Zhao, Edible films and coatings for shelf life extension of mango: a review, *Crit. Rev. Food Sci. Nutr.*, 2022, **62**(9), 2432–2459.
13 P. H. Huang, Y. J. Chen, Y. W. Lin and D. W. Huang, Gelatin-kappa-carrageenan-based edible film incorporated with ethanol extracts from Premna microphylla Turcz leaves for preservation of sailfish fillets, *LWT*, 2024, **208**, 116710.
14 Y. Li, X. Qi, C. Fan, Y. Fan, H. Zhang, J. Zhang, *et al.*, Novel synergistic cross-linking ameliorate ready-to-eat sea cucumber deterioration and its quantum chemical analysis, *Food Chem.*, 2024, **439**, 138097.
15 R. Kumar, G. Ghoshal and M. Goyal, Biodegradable composite films/coatings of modified corn starch/gelatin for shelf life improvement of cucumber, *J. Food Sci. Technol.*, 2021, **58**(4), 1227–1237.
16 S. Dehghani, S. V. Hosseini and J. M. Regenstein, Edible films and coatings in seafood preservation: A review, *Food Chem.*, 2018, **240**, 505–513.
17 T. R. Hashemi, S. M. Jafari, H. Mirzaei, A. Mohammadi Nafchi and D. Dehnad, Preparation and characterization of nano-SiO2 reinforced gelatin-k-carrageenan biocomposites, *Int. J. Biol. Macromol.*, 2018, **111**, 1091–1099.
18 F. He, Q. Kong, Z. Jin and H. Mou, Developing a unidirectionally permeable edible film based on κ-carrageenan and gelatin for visually detecting the freshness of grass carp fillets, *Carbohydr. Polym.*, 2020, **241**, 116336.
19 S. M. Alizadeh, M. Tavassoli, S. A. Salim, M. Azizi-lalabadi and D. J. McClements, Development of green halochromic smart and active packaging materials: TiO2 nanoparticle- and anthocyanin-loaded gelatin/κ-carrageenan films, *Food Hydrocoll.*, 2022, **124**, 107324.
20 S. Roy, P. Ezati and J. W. Rhim, Gelatin/Carrageenan-Based Functional Films with Carbon Dots from Enoki Mushroom for Active Food Packaging Applications, *ACS Appl. Polym. Mater.*, 2021, **3**(12), 6437–6445.
21 N. B. Rathod, S. P. Bangar, V. Šimat and F. Ozogul, Chitosan and gelatine biopolymer-based active/biodegradable packaging for the preservation of fish and fishery products, *Int. J. Food Sci. Technol.*, 2023, **58**(2), 854–861.
22 S. Roy and J. W. Rhim, Preparation of Gelatin/Carrageenan-Based Color-Indicator Film Integrated with Shikonin and Propolis for Smart Food Packaging Applications, *ACS Appl. Bio Mater.*, 2021, **4**(1), 770–779.
23 R. Mu, X. Hong, Y. Ni, Y. Li, J. Pang, Q. Wang, *et al.*, Recent trends and applications of cellulose nanocrystals in food industry, *Trends Food Sci. Technol.*, 2019, **93**, 136–144.
24 T. Ghosh, S. Roy, A. Khan, K. Mondal, P. Ezati and J. W. Rhim, Agricultural waste-derived cellulose nanocrystals for sustainable active food packaging applications, *Food Hydrocoll.*, 2024, **154**, 110141.
25 A. Khan, T. Huq, R. A. Khan, B. Riedl and M. Lacroix, Nanocellulose-Based Composites and Bioactive Agents for Food Packaging, *Crit. Rev. Food Sci. Nutr.*, 2014, **54**(2), 163–174.
26 P. Criado, C. Fraschini, S. Salmieri and M. Lacroix, Modification of Nanocrystalline Cellulose for Bioactive Loaded Films, *J. Res. Updates Polym. Sci.*, 2014, **3**(2), 122–135.
27 G. Lavrič, A. Oberlintner, I. Filipova, U. Novak, B. Likozar and U. Vrabič-Brodnjak, Functional Nanocellulose, Alginate and Chitosan Nanocomposites Designed as Active Film Packaging Materials, *Polymers*, 2021, **13**(15), 2523.
28 Z. Yu, F. K. Alsammarraie, F. X. Nayigiziki, W. Wang, B. Vardhanabhuti, A. Mustapha, *et al.*, Effect and mechanism of cellulose nanofibrils on the active functions of biopolymer-based nanocomposite films, *Food Res. Int.*, 2017, **99**, 166–172.
29 L. Jiang, Y. Han, X. Meng, Y. Xiao and H. Zhang, Cellulose Nanocrystals Reinforced Zein/Catechin/β-Cyclodextrin Inclusion Complex Nanoparticles Nanocomposite Film for Active Food Packaging, *Polymers*, 2021, **13**(16), 2759.
30 M. A. Hubbe, A. Ferrer, P. Tyagi, Y. Yin, C. Salas, L. Pal, *et al.*, Nanocellulose in Thin Films, Coatings, and Plies for Packaging Applications: A Review, *Bioresources*, 2017, **12**(1), 2143–2233.
31 G. Fotie, S. Limbo and L. Piergiovanni, Manufacturing of Food Packaging Based on Nanocellulose: Current Advances and Challenges, *Nanomaterials*, 2020, **10**(9), 1726.

32 C. Trilokesh and K. B. Uppuluri, Isolation and characterization of cellulose nanocrystals from jackfruit peel, *Sci. Rep.*, 2019, **9**(1), 16709.
33 L. K. Kurabetta, S. P. Masti, M. P. Eelager, M. N. Gunaki, S. Madihalli, A. A. Hunashyal, *et al.*, Physicochemical and antioxidant properties of tannic acid crosslinked cationic starch/chitosan based active films for ladyfinger packaging application, *Int. J. Biol. Macromol.*, 2023, **253**, 127552.
34 M. N. Gunaki, S. P. Masti, L. K. Kurabetta, J. P. Pinto, A. A. Hunashyal, N. P. Dalbhanjan, *et al.*, Influence of chitosan-capped quercetin nanoparticles on chitosan/poly(vinyl) alcohol multifunctional films: A sustainable approach for bread preservation, *Int. J. Biol. Macromol.*, 2025, **299**, 140029.
35 J. P. Pinto, O. J. D'souza, V. D. Hiremani, N. P. Dalbanjan, S. K. Praveen Kumar, S. S. Narasagoudr, *et al.*, Functional properties of taro starch reinforced polysaccharide based films for active packaging, *Food Biosci.*, 2023, **56**, 103340.
36 S. Madihalli, S. P. Masti, M. P. Eelager, R. B. Chougale, L. K. Kurabetta, A. A. Hunashyal, *et al.*, Quinic acid and montmorillonite integrated chitosan/pullulan active films with potent antimicrobial and barrier properties to prolong the shelf life of tofu, *Food Biosci.*, 2024, **62**, 105492.
37 L. K. Kurabetta, S. P. Masti, M. N. Gunaki, A. A. Hunashyal, M. P. Eelager, R. B. Chougale, *et al.*, A synergistic influence of gallic acid/ZnO NPs to strengthen the multifunctional properties of methylcellulose: A conservative approach for tomato preservation, *Int. J. Biol. Macromol.*, 2024, **277**, 134191.
38 L. K. Kurabetta, S. P. Masti, M. N. Gunaki, A. A. Hunashyal, R. B. Chougale, N. P. Dalbanjan, *et al.*, Exploration of physicochemical and biological properties of phenylalanine incorporated carboxymethyl cellulose/poly(vinyl alcohol) based bioactive films for food packaging applications, *Food Biosci.*, 2024, **61**, 104869.
39 M. P. Eelager, S. P. Masti, S. Madihalli, N. Gouda, L. K. Kurbetta, M. N. Gunaki, *et al.*, The effect of cetrimide crosslinking on biodegradable PVA/xanthan gum herbicidal films: Towards sustainable agriculture and its influence on soil fertility, *J. Environ. Chem. Eng.*, 2025, **13**(2), 116029.
40 J. P. Pinto, M. H. Anandalli, A. A. Hunashyal, M. S. P. Priyadarshini, R. B. Chougale, *et al.*, Carbon nanotubes reinforced chitosan/poly (1-vinylpyrrolidone-co-vinyl acetate) films: a sustainable approach for optoelectronic applications, *J. Mater. Sci.: Mater. Electron.*, 2025, **36**(17), 1035.
41 L. K. Kurabetta, S. P. Masti, M. N. Gunaki, A. A. Hunashyal, R. B. Chougale, N. P. Dalbanjan, *et al.*, Vanillin reinforced cationic starch/poly(vinyl alcohol) based antimicrobial and antioxidant bioactive films: sustainable food packaging materials, *Sustainable Food Technol.*, 2025, **3**(5), 1353–1364.
42 M. N. Gunaki, S. P. Masti, L. K. Kurabetta, S. Madihalli, A. A. Hunashyal, R. B. Chougale, *et al.*, Chitosan-encapsulated CuO nanoparticles reinforced multifunctional chitosan/gelatine nanocomposite films: A promising extension of cherry and grape shelf life, *J. Environ. Chem. Eng.*, 2025, **13**(5), 118397.
43 A. A. Hunashyal, S. P. Masti, L. K. Kurabetta, M. N. Gunaki, S. Madihalli, J. P. Pinto, *et al.*, Neem leaf-derived carbon dot-embedded chitosan-based active films: a sustainable approach to prolong the shelf life of prawns, *Sustainable Food Technol.*, 2025, **3**(6), 2088–2107.
44 A. A. Hunashyal, S. P. Masti, M. P. Eelager, O. J. D'souza, L. K. Kurabetta, M. N. Gunaki, *et al.*, Synergistic effects of Lantana camara leaf extract and in-situ AgNPs in chitosan/PVA films for lamb meat preservation, *Next Nanotechnol.*, 2025, **8**, 100292.
45 J. P. Pinto, M. B. Megalamani, A. A. Hunashyal, O. J. D′souza, S. T. Nandibewoor, S. P. Masti, *et al.*, Sustained drug delivery of the β-blocker acebutolol hydrochloride *via* chitosan–bilimbi leaf extract films, *RSC Pharm.*, 2026, **3**(1), 150–167.
46 M. Wei, M. Shan, L. Zhang, N. Chen, H. Tie, Y. Xiao, *et al.*, Preparation of gelatin/κ-carrageenan active films through procyanidins crosslinking: Physicochemical, structural, antioxidant and controlled release properties, *Food Hydrocoll.*, 2024, **153**, 110023.
47 M. Yadav and F. C. Chiu, Cellulose nanocrystals reinforced κ-carrageenan based UV resistant transparent bionanocomposite films for sustainable packaging applications, *Carbohydr. Polym.*, 2019, **211**, 181–194.
48 M. Yadav, K. Behera, Y. H. Chang and F. C. Chiu, Cellulose Nanocrystal Reinforced Chitosan Based UV Barrier Composite Films for Sustainable Packaging, *Polymers*, 2020, **12**(1), 202.
49 H. Wu, X. Wang, S. Li, Q. Zhang, M. Chen, X. Yuan, *et al.*, Incorporation of cellulose nanocrystals to improve the physicochemical and bioactive properties of pectin-konjac glucomannan composite films containing clove essential oil, *Int. J. Biol. Macromol.*, 2024, **260**, 129469.
50 S. Roy, P. Ezati and J. W. Rhim, Gelatin/Carrageenan-Based Functional Films with Carbon Dots from Enoki Mushroom for Active Food Packaging Applications, *ACS Appl. Polym. Mater.*, 2021, **3**(12), 6437–6445.
51 C. Cheng, S. Chen, J. Su, M. Zhu, M. Zhou, T. Chen, *et al.*, Recent advances in carrageenan-based films for food packaging applications, *Front. Nutr.*, 2022, **9**, 1004588.
52 M. Moustafa, A. Abu-Saied M, H. Taha T, M. Elnouby, E. A. El Desouky, S. Alamri, *et al.*, Preparation and Characterization of Super-Absorbing Gel Formulated from κ-Carrageenan–Potato Peel Starch Blended Polymers, *Polymers*, 2021, **13**(24), 4308.
53 A. Khan, Z. Riahi, J. T. Kim and J. W. Rhim, Gelatin/carrageenan-based smart packaging film integrated with Cu-metal organic framework for freshness monitoring and shelf-life extension of shrimp, *Food Hydrocoll.*, 2023, **145**, 109180.
54 M. Yadav, Y. K. Liu and F. C. Chiu, Fabrication of Cellulose Nanocrystal/Silver/Alginate Bionanocomposite Films with Enhanced Mechanical and Barrier Properties for Food Packaging Application, *Nanomaterials*, 2019, **9**(11), 1523.
55 S. Roy, H. J. Kim and J. W. Rhim, Synthesis of Carboxymethyl Cellulose and Agar-Based Multifunctional Films Reinforced

with Cellulose Nanocrystals and Shikonin, *ACS Appl. Polym. Mater.*, 2021, **3**(2), 1060–1069.

56 T. Ghosh, S. Roy, A. Khan, K. Mondal, P. Ezati and J. W. Rhim, Agricultural waste-derived cellulose nanocrystals for sustainable active food packaging applications, *Food Hydrocoll.*, 2024, **154**, 110141.

57 J. P. Pinto, M. B. Megalamani, A. A. Hunashyal, O. J. D′souza, S. T. Nandibewoor, S. P. Masti, *et al.*, Sustained drug delivery of the β-blocker acebutolol hydrochloride *via* chitosan–bilimbi leaf extract films, *RSC Pharm.*, 2026, **3**(1), 150–167.

58 J. P. Pinto, V. D. Hiremani, O. J. D'souza, S. Khanapure, S. S. Narasagoudr, N. Goudar, *et al.*, Development of Chitosan-Copovidone nanocomposite films with antioxidant and antibacterial properties for food packaging applications, *Food Human.*, 2023, **1**, 378–390.

59 J. P. Pinto, O. J. D'souza, V. D. Hiremani, N. P. Dalbanjan, S. K. Praveen Kumar, S. S. Narasagoudr, *et al.*, Functional properties of taro starch reinforced polysaccharide based films for active packaging, *Food Biosci.*, 2023, **56**, 103340.

60 N. Goudar, V. D. Hiremani, O. J. D'souza, J. P. Pinto, S. P. Masti and R. B. Chougale, Design and fabrication of polysaccharide based excellent chemical resistant and UV barrier ternary blend films for green packaging applications, *J. Food Sci. Technol.*, 2024, **61**(3), 481–490.

61 J. P. Pinto, M. H. Anandalli, A. A. Hunashyal, M. S. P. Priyadarshini, R. B. Chougale, *et al.*, Carbon nanotubes reinforced chitosan/poly (1-vinylpyrrolidone-co-vinyl acetate) films: a sustainable approach for optoelectronic applications, *J. Mater. Sci.: Mater. Electron.*, 2025, **36**(17), 1035.

62 Y. He, H. Li, X. Fei and L. Peng, Carboxymethyl cellulose/cellulose nanocrystals immobilized silver nanoparticles as an effective coating to improve barrier and antibacterial properties of paper for food packaging applications, *Carbohydr. Polym.*, 2021, **252**, 117156.

63 S. Ahammed, F. Liu, M. N. Khin, W. H. Yokoyama and F. Zhong, Improvement of the water resistance and ductility of gelatin film by zein, *Food Hydrocoll.*, 2020, **105**, 105804.

64 R. Zhang, X. Wang, J. Wang and M. Cheng, Synthesis and Characterization of Konjac Glucomannan/Carrageenan/Nano-silica Films for the Preservation of Postharvest White Mushrooms, *Polymers*, 2018, **11**(1), 6.

65 F. Sun, J. Zhao, P. Shan, K. Wang, H. Li and L. Peng, Gelatin-based composite film integrated with nanocellulose and extract-metal complex derived from coffee leaf for sustainable and active food packaging, *Food Hydrocoll.*, 2025, **159**, 110610.

66 M. He, Y. Huang, Z. Cui, W. Yao, J. Xu, Q. Li, *et al.*, Flexible and exceptional hemostatic chitin sponges with controllable structure and their properties, *Eur. Polym. J.*, 2025, **241**, 114405. Available from: https://linkinghub.elsevier.com/retrieve/pii/S0014305725006937.

67 Q. Gao, L. N. Guo, Li S. heng, W. Wu, J. W. Ding, H. J. Xu, *et al.*, Biodegradation mechanism of cellulose, hemicellulose, and lignin in bacteria-dominant aerobic composting from agricultural biomass waste:A review, *Carbohydr. Polym. Technol. Appl.*, 2025, **11**, 100879. Available from: https://linkinghub.elsevier.com/retrieve/pii/S2666893925002208.

68 E. Malekzadeh, A. Tatari and M. Dehghani Firouzabadi, Effects of biodegradation of starch-nanocellulose films incorporated with black tea extract on soil quality, *Sci. Rep.*, 2024, **14**(1), 18817.

69 G. A. Paula, N. M. B. Benevides, A. P. Cunha, A. V. de Oliveira, A. M. B. Pinto, J. P. S. Morais, *et al.*, Development and characterization of edible films from mixtures of κ-carrageenan, ι-carrageenan, and alginate, *Food Hydrocoll.*, 2015, **47**, 140–145.

70 J. S. Alves, K. C. dos Reis, E. G. T. Menezes, F. V. Pereira and J. Pereira, Effect of cellulose nanocrystals and gelatin in corn starch plasticized films, *Carbohydr. Polym.*, 2015, **115**, 215–222.

71 S. Nie, Q. Fu, X. Lin, C. Zhang, Y. Lu and S. Wang, Enhanced performance of a cellulose nanofibrils-based triboelectric nanogenerator by tuning the surface polarizability and hydrophobicity, *Chem. Eng. J.*, 2021, **404**, 126512.

72 H. Kono, E. Tsukamoto and K. Tajima, Facile Post-Carboxymethylation of Cellulose Nanofiber Surfaces for Enhanced Water Dispersibility, *ACS Omega*, 2021, **6**(49), 34107–34114.

73 M. F. Guimarães, L. Pighinelli, R. L. Paz, M. Kmiec, G. Zehetmeyer, C. M. Becker, *et al.*, Chemical and physical properties of nanocrystalline chitosan by the method: Modified nanochitosan complex and process of obtaining modified nanochitosan, *Carbohydr. Res.*, 2020, **493**, 108035.

74 M. El Achaby, Z. Kassab, A. Barakat and A. Aboulkas, Alfa fibers as viable sustainable source for cellulose nanocrystals extraction: Application for improving the tensile properties of biopolymer nanocomposite films, *Ind. Crops Prod.*, 2018, **112**, 499–510.

75 S. Roy, P. Ezati and J. W. Rhim, Gelatin/Carrageenan-Based Functional Films with Carbon Dots from Enoki Mushroom for Active Food Packaging Applications, *ACS Appl. Polym. Mater.*, 2021, **3**(12), 6437–6445.

76 L. Jiang, Y. Han, X. Meng, Y. Xiao and H. Zhang, Cellulose Nanocrystals Reinforced Zein/Catechin/β-Cyclodextrin Inclusion Complex Nanoparticles Nanocomposite Film for Active Food Packaging, *Polymers*, 2021, **13**(16), 2759.

77 J. Nam, Y. Hyun, S. Oh, J. Park, H. J. Jin and H. W. Kwak, Effect of cross-linkable bacterial cellulose nanocrystals on the physicochemical properties of silk sericin films, *Polym. Test.*, 2021, **97**, 107161.

78 S. M. Costa, D. P. Ferreira, P. Teixeira, L. F. Ballesteros, J. A. Teixeira and R. Fangueiro, Active natural-based films for food packaging applications: The combined effect of chitosan and nanocellulose, *Int. J. Biol. Macromol.*, 2021,

177, 241–251.

79 M. Yadav, K. Behera, Y. H. Chang and F. C. Chiu, Cellulose Nanocrystal Reinforced Chitosan Based UV Barrier Composite Films for Sustainable Packaging, *Polymers*, 2020, **12**(1), 202.

80 D. Zheng, S. Cao, D. Li, Y. Wu, P. Duan, S. Liu, *et al.*, Fabrication and characterization of chitosan/anthocyanin intelligent packaging film fortified by cellulose nanocrystal for shrimp preservation and visual freshness monitoring, *Int. J. Biol. Macromol.*, 2024, **264**, 130692.

81 C. Zhang, Y. Dan, J. Peng, L. Turng, R. Sabo and C. Clemons, Thermal and Mechanical Properties of Natural Rubber Composites Reinforced with Cellulose Nanocrystals from Southern Pine, *Adv. Polym. Technol.*, 2014, **33**(S1), DOI: 10.1002/adv.21448.